

## Deep arid system hydrodynamics

### 1. Equilibrium states and response times in thick desert vadose zones

Michelle A. Walvoord,<sup>1</sup> Mitchell A. Plummer,<sup>2</sup> and Fred M. Phillips

Earth and Environmental Science Department, New Mexico Institute of Mining and Technology, Socorro, New Mexico, USA

Andrew V. Wolfsberg

Earth and Environmental Sciences Division, Los Alamos National Laboratory, Los Alamos, New Mexico, USA

Received 6 August 2001; revised 21 April 2002; accepted 21 April 2002; published 20 December 2002.

[1] Quantifying moisture fluxes through deep desert soils remains difficult because of the small magnitude of the fluxes and the lack of a comprehensive model to describe flow and transport through such dry material. A particular challenge for such a model is reproducing both observed matric potential and chloride profiles. We propose a conceptual model for flow in desert vadose zones that includes isothermal and nonisothermal vapor transport and the role of desert vegetation in supporting a net upward moisture flux below the root zone. Numerical simulations incorporating this conceptual model match typical matric potential and chloride profiles. The modeling approach thereby reconciles the paradox between the recognized importance of plants, upward driving forces, and vapor flow processes in desert vadose zones and the inadequacy of the downward-only liquid flow assumption of the conventional chloride mass balance approach. Our work shows that water transport in thick desert vadose zones at steady state is usually dominated by upward vapor flow and that long response times, of the order of  $10^4$ – $10^5$  years, are required to equilibrate to existing arid surface conditions. Simulation results indicate that most thick desert vadose zones have been locked in slow drying transients that began in response to a climate shift and establishment of desert vegetation many thousands of years ago. **INDEX TERMS:** 1866 Hydrology: Soil moisture; 1875 Hydrology: Unsaturated zone; **KEYWORDS:** modeling, vapor flow, chloride, matric potential

**Citation:** Walvoord, M. A., M. A. Plummer, F. M. Phillips, and A. V. Wolfsberg. Deep arid system hydrodynamics. 1. Equilibrium states and response times in thick desert vadose zones. *Water Resour. Res.*, 38(12), 1308, doi:10.1029/2001WR000824, 2002.

#### 1. Introduction

[2] Rising pressures of population in arid and semiarid regions necessitate better quantification of interdrainage fluxes through desert floors and better prediction of how these fluxes may vary over timescales of human interest. Is there significant downward moisture movement through interdrainage desert floor environments that will recharge the aquifers below [Gee and Kirkham, 1984; Stone, 1984; Stone and McGurk, 1985; Stephens and Knowlton, 1986; Stephens, 1994]? Or do thick vadose zones serve as effective barriers to moisture flow and contaminant migration from the surface or from a repository to the water table [Wagner, 1981; Relth and Thompson, 1992]? The initial step in addressing these questions involves understanding the processes that control moisture flux regimes in desert vadose zones and the timescales on which these processes operate. Current soil water fluxes within arid unconsoli-

dated vadose zones in interdrainage areas (regions away from channels and arroyos) are generally thought to be very low [Scanlon *et al.*, 1999], perhaps negligible below the soil root zone.

[3] In this study, we examine the existing conceptual models invoked to explain matric potential and chloride profiles measured in deep desert vadose zones and offer an alternative that better matches observed data. Our model incorporates vapor transport and uses observations of temporally invariant matric potentials at 3–5 m depths (over ~5 year monitoring periods) [Andraski, 1997; Scanlon *et al.*, 1999] as a basis for specifying a fixed subroot zone matric potential condition. By employing this condition, our model avoids adopting the common assumption of downward-only advection to describe the flow regime.

#### 1.1. Steady State Models: Hydrostatic Equilibrium and Unit Gradient

[4] Soil water moves in response to a hydraulic potential gradient comprised predominantly of the following components: the gravitational potential ( $z$ ), the matric (or pressure) potential ( $\psi$ ), and the osmotic potential ( $\psi_o$ ) [Hillel, 1980]. The elevation above a reference level, generally designated as the water table, defines the gravitational potential. The

<sup>1</sup>Now at U.S. Geological Survey, Lakewood, Colorado, USA.

<sup>2</sup>Now at Idaho National Engineering and Environmental Laboratory, Idaho Falls, Idaho, USA.

U.S. NUCLEAR REGULATORY COMMISSION

In the Matter of Louisiana Energy Services, L.P.

Docket No. 70-3103 Official Exhibit No. LES

OFFERED by Applicant/Licensee Intervenor \_\_\_\_\_

NRC Staff \_\_\_\_\_ Other \_\_\_\_\_

IDENTIFIED on 2/2/05 Witness/Panel Harper/Peery

Action Taken: ADMITTED REJECTED WITHDRAWN

Reporter/Clerk Barbara Engel

DOCKETED  
USNRC

2005 MAR -3 PH 3: 07

OFFICE OF THE SECRETARY  
RULES AND ADJUDICATIONS  
ADJUDICATIONS STAFF

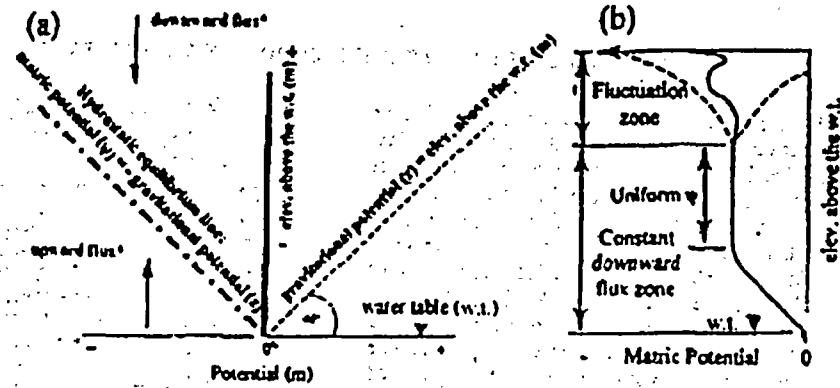


Figure 1. (a) Conventional hydrostatic equilibrium model (modified from Figure 3.2 from the National Research Council [1995] Ward Valley report). (b) Unit gradient model (modified from Figure 1 in Nimmo et al. [1994]).

matric potential describes the interaction between the liquid and the solid matrix. Capillary and adsorptive forces attract and bind water to the matrix, thereby reducing the potential energy below that of bulk water [Hillel, 1980]. By convention, matric potentials in unsaturated soil (i.e., below the reference atmospheric pressure) are negative and become increasingly negative as the soil dries [Stephens, 1996]. The osmotic potential describes the reduction of soil water vapor pressure due to the presence of solutes. Osmotic potentials are generally much smaller than matric potentials in arid vadose zones [Walvoord, 2002].

[5] Two common conceptual models that address vadose zone potentials are the conventional hydrostatic equilibrium model and the unit gradient model. According to the hydrostatic equilibrium model (also termed static fluid distribution and gravity capillary equilibrium) presented in text books [i.e., Bear, 1972; Koorevaar et al., 1983; Jury et al., 1991; Looney and Falta, 2000a, 2000b] and papers on desert vadose zone hydrology [i.e., National Research Council (NRC), 1995; Scanlon et al., 1999; Scanlon, 2000], no-flow conditions result when the matric potential ( $\psi$ ) equally balances the gravitational potential ( $z$ ) (Figure 1a). Assuming steady state conditions, matric potentials that plot below the hydrostatic equilibrium line in Figure 1a indicate upward flow, and matric potentials that plot above indicate downward flow. If the hydrostatic equilibrium model is adequate,

we would expect observed  $\psi$  profiles to plot close to the hydrostatic equilibrium line if water fluxes through desert soils in interdrainage regions are very small.

[6] The unit gradient model postulates that matric potentials below the active root zone contribute little to the total hydraulic gradient, exhibiting a zone of  $\psi$  as illustrated on the hypothetical profile in Figure 1b. Accordingly, the hydraulic gradient below the root zone, or shallow  $\psi$  fluctuation zone, equals unity in the vertical downward direction and the downward soil water flux equals the unsaturated hydraulic conductivity [Gardner, 1967; Nimmo et al., 1994]. Given a uniform soil profile, the steady state unit gradient model predicts that the downward flux below the root zone equals the flux across the water table interface, or recharge rate [Stephens, 1996].

[7] Measured matric potentials from thick vadose zones in the arid southwestern United States deviate from the linear profile predicted by the hydrostatic equilibrium model and from a uniform profile required for the unit gradient model. Observed desert vadose zone  $\psi$  profiles from interdrainage areas are typically curved, with extremely negative  $\psi$  near the surface and an exponential increase with depth (Figure 2). Comparison of observed  $\psi$  profiles to their corresponding hydrostatic equilibrium line in Figure 2 demonstrates a pattern of divergent flux. The slopes of the total potentials indicate an upward hydraulic gradient in the

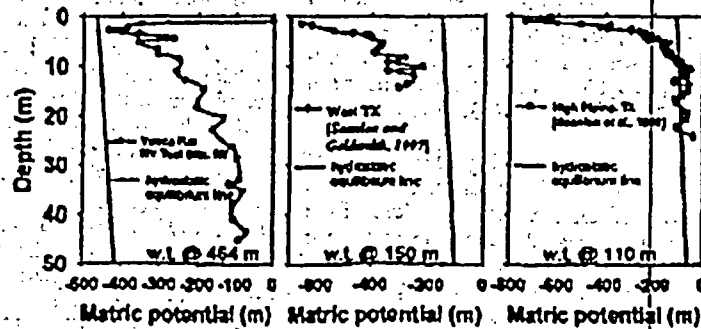


Figure 2. Vadose zone  $\psi$  profiles under desert floor environments in Nevada and west Texas.

upper profile and a downward hydraulic gradient below. Capillary forces draw soil water upward and dominate flow processes to depths of about 10–30 m in the profiles depicted in Figure 2. Below, the hydraulic gradient reverses, and soil water drains by gravity. Similarly, Scanlon *et al.* [1997] report that  $\psi$  measurements in interdrainage areas of many basins in the southwest generally indicate an upward driving force for water movement in the top 20 to 40 m. The divergent flux pattern raises several concerns, the most obvious regarding the equilibrium state of the profile. The lack of a moisture source to supply fluxes at the plane of divergence located deep in the profile raises questions regarding the merit of a steady state assumption. An alternative assumption is that the divergent moisture flux pattern reflects a temporary phenomenon resulting from transient flow processes [Scanlon, 2000]. A transient interpretation evokes several questions. What are typical hydraulic response times associated with thick desert vadose zones? And, to what depths do seasonal surface transients actually propagate? The study presented here explicitly addresses the former question. Long-term monitoring studies address the latter question and report minimal temporal variability in  $\psi$  measurements below depths of ~3–5 m under desert vegetation [e.g., Enfield *et al.*, 1973; Fischer, 1992; Andraski, 1997; Scanlon *et al.*, 1999]. During a 5-year monitoring period, Andraski [1997] observed that  $\psi$  under vegetated sites in the Mojave Desert remained between -600 m to -400 m at 1.55 to 4.5 m depth. Vegetated desert vadose zones below a few meters appeared to be buffered from diurnal and seasonal surface transients at least on the decadal timescale.

[8] Application of the unit gradient conceptual model to the observed profiles implies that the zone of upward liquid flux in Figure 2 is only a temporary phenomenon (i.e., part of the seasonal or longer-term variations in the upper vadose zone). This would require, however, that the active root zone, where changes in soil moisture storage are readily affected, extends to more than 10 m below the surface. Although some desert vegetation species have been documented to extend their roots to depths of 15 to 25 m [Canadell *et al.*, 1996], it is unlikely that an active rooting zone depth of this magnitude is ubiquitous over the biogeographical range of sites where these types of  $\psi$  profiles are measured. Canadell *et al.* [1996] reports an average maximum root depth in deserts of  $5.2 \pm 0.8$  m. The unit gradient conceptual model also suffers from the lack of a moisture source to supply the downward flux unless episodic infiltration reaches depths of  $\geq 10$  m, a supposition contrary to observations [e.g., Enfield *et al.*, 1973; Fischer, 1992; Andraski, 1997].

[9] Despite the noted concerns regarding the application of the hydrostatic equilibrium and unit gradient models to deep desert vadose zone  $\psi$  profiles, direct interpretations of the data in Figure 2 suggest net upward water movement in the depth interval from 3 to ~10 or 20 m. Yet, when applying the conventional chloride mass balance set of equations, a downward-only advective flux of liquid is assumed.

## 1.2. Transient Conceptual Models: Reduced Recharge and Zero Recharge

[10] Chloride, deposited on the ground surface in wind-blown fallout and precipitation, serves as an environmental

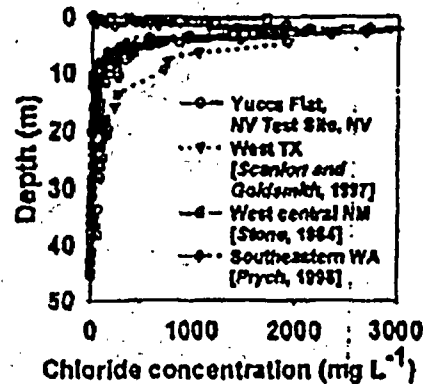


Figure 3. Vadose zone chloride profiles under desert floor environments in the western United States. Chloride values are reported as pore water concentrations.

tracer commonly used to quantify soil water fluxes and ages based on mass balance [Allison, 1988; Cook *et al.*, 1992; Allison *et al.*, 1994; Phillips, 1994; Frudic, 1994; Wood, 1999]. As water leaves the soil via evapotranspiration, chloride remains, thereby increasing the pore water concentration. Greater chloride values thus correspond to lower soil water fluxes. Assumptions employed with the simple chloride mass balance (CMB) approach include: (1) chloride is derived from atmospheric sources only, (2) chloride moves through the soil profile by one-dimensional downward advection, and (3) the chloride deposition rate is constant. These simplifying assumptions lead to uncertainties in CMB age and flux estimates [Murphy *et al.*, 1996; Ginn and Murphy, 1997; Scanlon *et al.*, 1997; Scanlon, 2000].

[11] An idealized chloride profile under steady piston flow conditions with extraction of water by roots would be characterized by concentrations increasing with depth through the root zone to a uniform value below the root zone. Measured chloride profiles from arid vadose zones in the southwestern United States deviate from the idealized profile and typically display a shallow bulge containing very high concentrations and much lower, relatively uniform concentrations at depth (Figure 3). Departure from the idealized profile records a violation of the steady flow assumption [Wood, 1999]. Observed chloride inventories contained within the shallow bulge often correspond to ~15 kyr of accumulation based on long-term average estimates of chloride deposition [Phillips, 1994]. Substantial evidence supports a climate shift from cool, wet conditions to warmer, drier conditions at 12–15 ka in the southwestern United States [Benson *et al.*, 1990; Morrison, 1991; Phillips *et al.*, 1992; Allen and Anderson, 1993]. Accordingly, several studies attribute the character of the chloride bulge measured in southwestern United States vadose zones (Figure 3) to this well-documented paleoclimatic transition [Scanlon, 1991; Phillips, 1994]. Presumably, the shift to lower precipitation rates and warmer temperatures brought about a reduction in the amount of soil moisture percolating through the root zone. This “reduced-recharge conceptual model” posits that the climate shift translated to a lesser downward soil water surface flux resulting in much greater

chloride concentrations at shallow depths relative to those found deep in the profile. A more extreme variant of that explanation that could be termed the "zero-recharge model" proposes that no soil water has percolated below the root zone since the arid climate shift at 12–15 ka, resulting in the accumulation of significant amounts of chloride within the root zone.

[12] In addition to estimating soil water ages, the CMB equations are also used to quantify current soil water fluxes (below the region of chloride accumulation) (Phillips, 1994; Scanlon, 2000) and paleofluxes (Phillips, 1994; Tyler *et al.*, 1996). CMB estimates of past and present fluxes apply to the reduced-recharge conceptual model. More dilute chloride concentrations deeper in the profile reflect greater soil water fluxes associated with a wetter past climate, whereas the greater chloride concentrations within the bulge reflect much less percolation past the root zone under the current arid climate. Adoption of the zero-recharge conceptual model limits the CMB application to estimates of paleofluxes and chloride ages below the base of the chloride bulge.

### 1.3. Disparity Between $\psi$ and Chloride Vadose Zone Profile Interpretations

[13] The reduced-recharge and zero-recharge conceptual models invoked to explain vadose zone chloride profiles do not adequately explain the corresponding  $\psi$  profiles that indicate upward fluxes in the upper 10 plus meters. Resolution of this apparent disparity serves as our primary objective in developing an improved conceptual model. The assumption of downward-only advection employed to quantify soil water fluxes using the CMB equations and the unit gradient model approach (Nimmo *et al.*, 1994) necessarily produces positive estimates of recharge. Such estimates may support the idea that diffuse recharge across extensive areas of arid and semiarid regions significantly contributes to the overall basin-scale water balance. Stephens (1994) provides a summary table of diffuse recharge estimates from 17 previous studies that range from 0 to 100 mm yr<sup>-1</sup> at semiarid and arid sites. Although the methods employed for quantifying the fluxes included physical and chemical approaches, all analyses assumed downward flow in the deep profile. In contrast, the zero-recharge conceptual model assumes no flow past the root zone or through the deeper profile. A new conceptual and numerical model, developed and tested in the next section, provides a basis for us to challenge the assumptions of downward advection or zero flow to describe the moisture flow regime in deep desert vadose zones.

## 2. Deep Arid System Hydrodynamic Model

### 2.1. Conceptual Model

[14] The estimated ages of chloride bulge inventories in the southwestern United States indicate a link with the timing of the Holocene-Pleistocene climate shift at 12–15 ka. However, the paleoclimatic explanation alone fails to explain the  $\psi$  data from deep profiles that contain the characteristic chloride bulge. Therefore we propose that the transition to a warmer and drier climate and the replacement of mesic vegetation by xeric (desert) vegetation induced the development and maintenance of very negative

$\psi$  in the soil at the base of the root zone. Accordingly, the effects of episodic infiltration events are dampened in the near-surface soil and do not influence the deeper vadose flow regime. Desert vegetation has been shown to be capable of extracting soil moisture under soil  $\psi$  conditions as dry as -800 m (Odensing *et al.*, 1974) and to be resistant to xylem cavitation under soil  $\psi$  conditions as dry as -400 m to -1000 m (Pockman *et al.*, 1995). Multiyear lysimeter studies from three arid sites investigated by Gee *et al.* (1994) suggested that vegetation is the primary factor controlling the water balance. Gee *et al.* (1994) found that desert vegetation eliminated deep infiltration over the monitoring period at the southwestern United States sites. The lysimeter results from Gee *et al.* (1994) are consistent with the absence of seasonal  $\psi$  transients propagating below depths of about 3–5 m under desert vegetation, based on studies in which  $\psi$  was continuously measured by in-situ soil psychrometers. [e.g., Fischer, 1992; Andraski, 1997; Scanlon *et al.*, 1999]. Andraski (1997) reported that moisture from precipitation that accumulates in the upper 75 cm is removed by evapotranspiration on a seasonal basis, and that seasonal  $\psi$  variation remain confined to depths above 4 m at the vegetated Beatty, NV site. Although these studies obviously cannot demonstrate that  $\psi$  at depths of ~4 m have remained constant over the past 10–15 kyr, they do support a key assumption that  $\psi$  in deep desert root zones do not exhibit significant seasonal changes as might be expected based on precedents from vadose zone studies in humid regions [i.e., Johnston, 1987]. In addition to the fixed subroot zone  $\psi$  condition, our conceptual model, which we term the Deep Arid System Hydrodynamic (DASH) model, incorporates a temperature profile described by the mean annual geothermal gradient and includes the effect of both temperature and  $\psi$  on vapor density and vapor flux. Liquid and vapor can move both upward and downward, and at different rates and opposing directions from each other. In assuming a fixed subroot zone  $\psi$  condition, the DASH conceptual model does not attempt to capture the seasonal moisture flux dynamics in the upper few meters. Those dynamics would include, for example, the net downward vapor flux in the upper ~1 meter of soil that should result from seasonal temperature variations (Milly, 1996).

### 2.2. Mathematical and Numerical Model

[15] We use the finite element heat and mass transfer (FEHM) (Zvoloski *et al.*, 1997) computer code for simulating unsaturated flow and transport in accordance with the DASH, reduced-recharge, and zero-recharge conceptual models. FEHM simulates nonisothermal, multiphase, multi-component flow in porous media. FEHM incorporates vapor transport driven by changes in vapor density resulting from a temperature gradient (thermal vapor flux component) and from a  $\psi$  gradient (isothermal vapor flux component). The van Genuchten relative permeability function (van Genuchten, 1980) describes the relationships between permeability and saturation and between pressure and saturation. (Further model description is included in the appendix). Assumptions inherent in FEHM include: (1) Darcy's Law appropriately describes the movement of liquid and vapor, (2) local thermal equilibrium between the fluid and the rock is maintained, and (3) solute transport does not affect the transfer of fluid or heat. Additional

Table 1. Input Parameters Used to Describe Properties and Conditions of the Model Domain for the Base Case

Parameter	Value
Soil texture	well-sorted sand
Porosity	45%
Thermal conductivity	$2.5 \text{ W m}^{-1} \text{ }^\circ\text{C}^{-1}$
Particle density	$2500 \text{ kg m}^{-3}$
Specific heat	$1000 \text{ J kg}^{-1} \text{ }^\circ\text{C}^{-1}$
Saturated permeability	$10^{-11} \text{ m}^2$
van Genuchten parameters $n$ and $m$	$4.5 \text{ m}^{-1}, 1.9$
Residual and maximum saturations	10%, 96%
Geothermal gradient	$35^\circ\text{C km}^{-1}$
Water table depth	200 m
Depth of fixed subroot zone $\psi$	4 m
Effective solute diffusion coefficient	$10^{-11} \text{ m}^2 \text{ s}^{-1}$

assumptions imposed in this study, but not inherent to FEHM, include (1) 1-D vertical flow adequately represents the hydrodynamics, (2) air flow is negligible, (3) chloride behaves conservatively (nonsorbing and nonreactive) and is nonvolatile, and (4) fractures, macropores, or other preferential flow paths do not affect the system. Chloride is assumed not to exit the soil through plant water uptake since most plants exclude chloride when absorbing water through the roots [Gardner, 1967].

### 2.3. Input Parameters, Boundary Conditions, and Initial Conditions

[16] A 200-m vertical column represents the physical system, a generalized alluvium vadose zone, used for testing conceptual models of 1-D nonisothermal, multiphase flow and transport in arid regions. The input parameter values designated as the "base case" are given in Table 1. The top of the vertical column represents the ground surface, and the bottom of the column represents the water table. Temperature gradients result from specifying temperatures at the top and bottom boundaries of  $18^\circ\text{C}$  and  $25^\circ\text{C}$ , based on a mean annual surface temperature in the desert southwestern United States (top boundary) and an average geothermal gradient of  $35^\circ\text{C km}^{-1}$  [Blankenship and Weir, 1973] (Ross [1984] uses  $30^\circ\text{C km}^{-1}$ ). Base case soil properties describe a homogenous sandy soil texture (Table 1). A residual saturation of 10% is consistent with data from alluvial material at the Nevada Test Site [Walvoord et al., 2002]. At low saturations near the base case residual saturation (i.e., 4.5% moisture content), the effective chloride diffusivity is  $\sim 10^{-11} \text{ m}^2 \text{ s}^{-1}$  [Conca and Wright, 1992; Schaefer et al., 1995].

[17] Initially, the system is set at a uniform downward liquid flux of  $10 \text{ mm yr}^{-1}$ , past the root zone, representative of a relatively wet climate [Tyler et al., 1996]. The initial solute profile consists of a uniform chloride pore water concentration of  $10 \text{ mg L}^{-1}$ . A prescribed solute flux of  $100 \text{ mg m}^{-2} \text{ yr}^{-1}$  at the surface boundary simulates continuous chloride deposition (Table 2). This prescribed flux represents both dry and wet chloride deposition and is a typical present-day value in the U.S. southwest [Dettinger, 1989]. We assume that although the relative contributions of dry and wet chloride deposition vary over time in response to climate changes, the total chloride flux, mainly controlled by distance to its oceanic source [Lunge and Werby, 1957], remains constant. Implementing the DASH conceptual model, a switch to a dry climate is simulated by specifying an average precipitation rate of  $200 \text{ mm yr}^{-1}$  at the surface (not past the root zone) and imposing a fixed  $\psi$  at 4 m depth, in accordance with observations from root zones underlying desert vegetation [Andraski, 1997; Scanlon et al., 1999]. The fixed subroot zone  $\psi$  condition distinguishes the DASH model from the reduced-recharge and zero-recharge models in these simulations.

### 2.4. Testing the Dash Model Against Previous Conceptual Models

[18] The DASH model is tested against the reduced-recharge and zero-recharge models by comparing results from simulations run for the fixed subroot zone  $\psi$  condition to results from a reduced-flux boundary condition of  $0.1 \text{ mm yr}^{-1}$  and a zero-flux boundary condition (Table 2). The simulations proceed for 15 kyr subsequent to the transition from the initial downward flux steady state to the imposed arid conditions identified with each conceptual model. The 15 kyr run-time criterion is based on typical measured chloride inventories in southwestern United States chloride bulges [Phillips, 1994]. Modeled  $\psi$  and chloride profiles for the DASH and reduced-recharge and zero-recharge conceptual models (Figures 4 and 5) are compared to typical observed profiles (Figures 2 and 3). The reduced-recharge model produces a much less negative  $\psi$  profile (Figure 4a) and a broader chloride profile (Figure 4b) than the observed profiles (Figures 2 and 3). The zero-recharge model produces peaked chloride profiles, resembling observed profiles, but generates much less negative matric potentials than commonly observed. In contrast, both the  $\psi$  and chloride profiles generated for the DASH model closely resemble the observed profiles, thereby favoring the DASH conceptual

Table 2. Initial and Boundary Conditions for Testing the Three Conceptual Models<sup>a</sup>

Conceptual Model	Initial condition All	Boundary condition Reduced Recharge	Boundary Condition Zero Recharge	Subroot Zone Condition DASH
Surface water flux				
Net infiltration	$10 \text{ mm yr}^{-1}$	$0.1 \text{ mm yr}^{-1}$	$0.001 \text{ mm yr}^{-1}$	N/A
Precipitation	N/A	N/A	N/A	$200 \text{ mm yr}^{-1}$
Subroot zone $\psi$	N/A	N/A	N/A	-400 m
Water table $\psi$	0 m	0 m	0 m	0 m
Surface temperature	$18^\circ\text{C}$	$18^\circ\text{C}$	$18^\circ\text{C}$	$18^\circ\text{C}$
Water table temperature	$25^\circ\text{C}$	$25^\circ\text{C}$	$25^\circ\text{C}$	$25^\circ\text{C}$
Chloride flux	$100 \text{ mg m}^{-2} \text{ yr}^{-1}$			
Source chloride concentration	$10 \text{ mg L}^{-1}$	$1 \text{ g L}^{-1}$	$100 \text{ g L}^{-1}$	$0.5 \text{ mg L}^{-1}$

<sup>a</sup> Initial conditions are the same for all three test simulations. N/A is not applied.

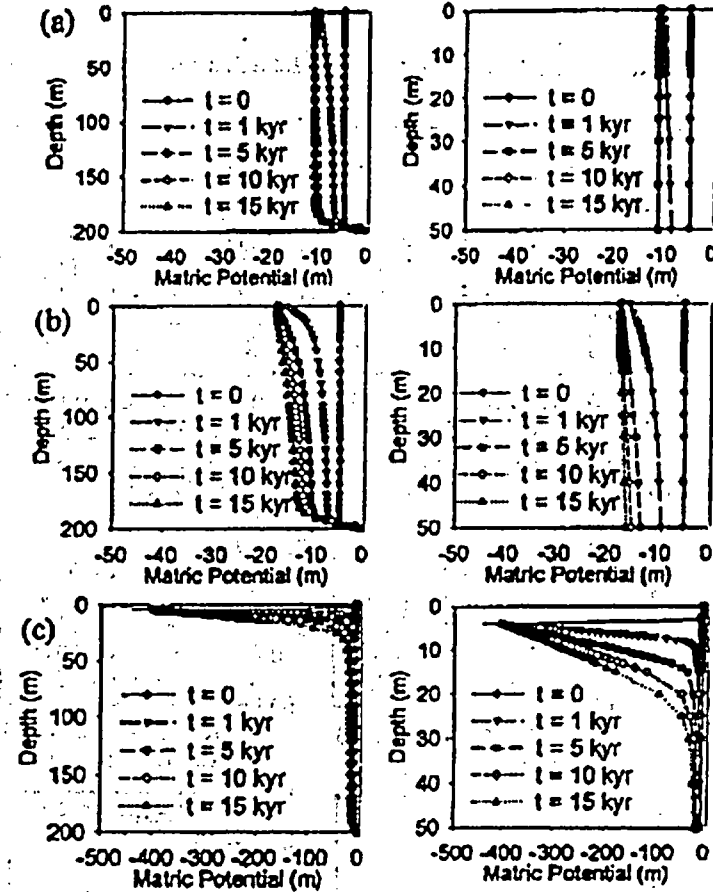


Figure 4. Numerically simulated  $\psi$  profiles for the (a) reduced-recharge, (b) zero-recharge, and (c) DASH conceptual models. The left graphs display the entire 200 m thick vadose zone, and right graphs show only the upper 50 m.

model over the reduced-recharge and zero-recharge conceptual models.

### 2.5. Current Transient State

[19] The DASH model moisture flux profiles below 4 m for the base case at 15 kyr from the switch to a drier climate represent the current conditions and indicate divergent liquid and net moisture fluxes and upward vapor fluxes (Figure 6). The upward geothermally driven vapor flux is sourced by evaporation from the water table. The upward isothermal vapor flux contributes significantly to drying in the upper 25 m. Between 4 and 25 meters, vapor fluxes exceed the liquid flux by at least an order of magnitude due to the very dry conditions and thus low unsaturated permeability. Liquid flows upward in the upper 13 m and downward below. Downward liquid fluxes below 13 m increase with depth as a result of the divergent drying process. Calculated liquid and vapor fluxes in the region below the fixed subroot zone  $\psi$  and above the water table are extremely small, on the order of  $10^{-3}$  mm yr $^{-1}$  (Table 3). In contrast to the very small fluxes predicted using the DASH model concept, the CMB approach based

on the reduced-recharge conceptual model, yields larger downward fluxes below the root zone and across the water table interface (Table 3). Furthermore, the DASH model flux distribution that reflects the current condition (Figure 6) illustrates that the net moisture flux below the root zone is not equivalent in magnitude or direction to the flux across the water table interface. The moisture flux distribution clearly violates the key steady state assumption for the conventional hydrostatic equilibrium and the unit gradient models. The moisture flux distribution also contests the stagnant condition assumption for the zero-recharge model. The transient state of vadose zone profiles given 15 kyr to approach equilibrium with the fixed root zone  $\psi$  condition suggests an extremely slow response of the system.

### 2.6. Hydrodynamic Equilibrium State

[20] Simulations carried to steady state using the DASH model and the base case set of parameters yield important insight into the equilibrium state of deep vadose zones and response to an arid climate shift. The lack of similarity between the DASH model-generated, steady state  $\psi$  profile

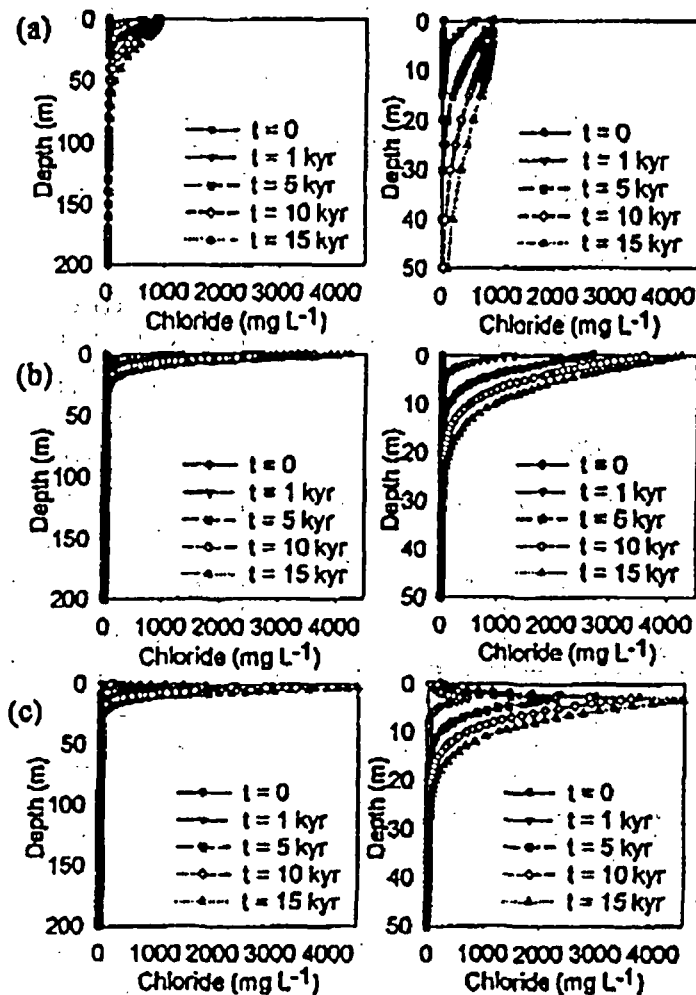


Figure 5. Numerically simulated chloride profiles for the (a) reduced-recharge, (b) zero-recharge, and (c) DASH conceptual models. The left graphs display the entire 200 m thick vadose zone and right side graphs show only the upper 50 m.

and the  $\psi$  profile required for the steady state conventional hydrostatic equilibrium model reveals a major misconception in conventional unsaturated flow theory as applied to desert vadose zones (Figure 7a). The DASH model produces a curved  $\psi$  profile at steady state (convex upward) similar to measured  $\psi$  profiles (Figure 2). The curvature indicates a divergent liquid flow pattern in which liquid fluxes are upward in the upper vadose zone and downward below. The moisture flux profiles show how a divergent liquid flow pattern can describe a steady state, net upward flux regime (Figure 7b). The upward thermal vapor flux, sourced by evaporation from the water table, decreases with height above the water table due to the decreasing temperature and vapor density gradients. To maintain equilibrium, vapor condenses and supplies a downward liquid flux in the deep vadose zone. Above some depth ( $\sim 90$  m for the base case), capillary forces, resulting from the specified subroot zone  $\psi$ , exceed gravitational forces imparted to the liquid,

and the liquid flux direction shifts to upward. The upward liquid flux in the shallow vadose zone is extremely small due to the dry conditions and very low unsaturated permeability. The equilibrium state is characterized by dynamic interaction between vapor and liquid fluxes summing to a net upward uniform moisture flux of  $\sim 0.012$  mm yr $^{-1}$  for the base case.

[2] The transient history of the base case simulation carried to steady state suggests a very slow response of deep vadose zones to an arid climate/xeric vegetation shift. Modeled steady state matric potential profiles that appear similar in character, in both shape and magnitude, to measured profiles could suggest that observed desert vadose zones are in equilibrium with current surface arid conditions. However, examination of the response times associated with the modeled steady state profiles suggests the contrary. We use the time required to complete an e-fold ( $1 - e^{-1}$  or 63% response from initial to final state) change in

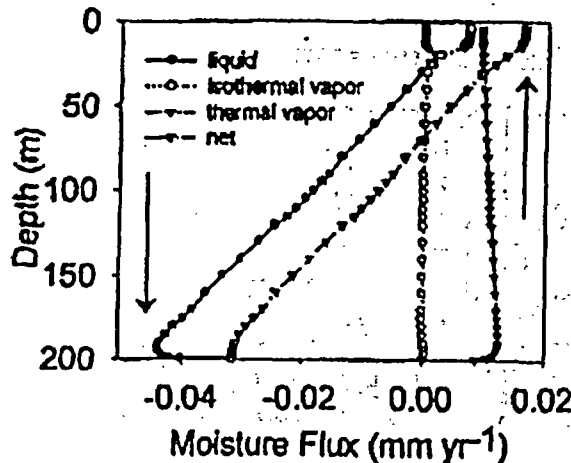


Figure 6. Moisture flux profile (below 4 m) at 15 kyr subsequent to the shift from steady downward flux conditions to a fixed subroot zone  $\psi$  condition (DASH model). Negative values indicate downward fluxes.

the matric potential profile to define the equilibrium response. The calculated response time of 80 kyr exceeds typical timescales of long-term climate change, which are on the order of 10 to 15 kyr. Consequently, we would expect deep desert vadose zones with similar parameters as the base case to still be in a very slow transition toward steady state, but nevertheless to be far from the "true" steady state.

[22] The moisture flux results (Figure 7b) show that vapor transport controls the hydrodynamics at steady state. Comparison of steady state  $\psi$  profiles for a fixed subroot zone  $\psi$  of  $-200$  m generated with and without isothermal vapor flux, thermal vapor flux and total vapor flux emphasizes this point (Figure 8). The hydrostatic equilibrium linear profile describes the steady state if the thermal vapor flux is neglected, regardless of whether or not the isothermal flux is considered. In contrast, curved  $\psi$  profiles describe the nonisothermal steady state, because the nonuniform thermal vapor flux requires a compensating moisture flux. The  $\psi$  profile displays more acute curvature (defined here as degree of deviation from the linear profile) in the absence of an isothermal vapor flux (Figure 8), and thus describes a wetter steady state. Without the isothermal vapor flux, all of the moisture liberated by the decreasing (with temperature and height above the water table) thermal vapor flux condenses and supplies a nonuniform downward liquid flux. However, when isothermal vapor effects are incorpo-

rated, some of the moisture liberated by the decreasing vapor flux is drawn upward and out of the system through the subroot zone sink, resulting in a drier steady state.

### 3. Sensitivity Analysis

[23] We perform a sensitivity analysis by systematically varying parameters and comparing results to the base case solution. The sensitivity analysis serves three purposes. First, varying parameters within a typical range of measured values helps evaluate whether the DASH model broadly applies to desert vadose zones or is narrowly limited to special cases. Second, results from a sensitivity analysis indicate which parameters exert primary influence on flow and transport in deep desert vadose zones. Such an evaluation may channel future research efforts to better characterize the more sensitive parameters. And third, the range of responses obtained through the sensitivity analysis provides a basis for assessing the uncertainty associated with applying the DASH conceptual model to field sites at which several key parameters may be poorly constrained. Variables considered in the sensitivity analyses include geothermal gradient, soil type (Table 4), water table depth, specified subroot zone  $\psi$  and vapor diffusion rate. Simulations carried to steady state generate a range of response times associated with each variable.

#### 3.1. Geothermal Gradient

[24] Since the base case moisture flux solution using the DASH model demonstrates the importance of thermal vapor transport at steady state, we expect the magnitude of the geothermal gradient to exert a major control on the equilibrium state of deep desert vadose zones. Simulation results from zero ( $0^\circ\text{C km}^{-1}$ ) and low ( $15^\circ\text{C km}^{-1}$ ) through high ( $65^\circ\text{C km}^{-1}$ ) geothermal gradients [e.g., Blankenbagen and Weir, 1973] corroborate this expectation (Figure 9). Increasing geothermal gradients induce greater thermal vapor fluxes, thereby reducing the depth of liquid flux divergence and enhancing the curvature of the  $\psi$  profile. The larger net upward moisture fluxes associated with higher geothermal gradients result in faster response times (Table 5). The zero geothermal gradient case produces a nearly linear  $\psi$  profile (Figure 9).

#### 3.2. Hydraulic Properties

[25] To assess the steady state flow regimes and response times for various soil types, we compare simulation results for sand (base case), silt, and silty clay. Saturated hydraulic permeability and van Genuchten fitting parameters are varied (Table 4), whereas thermal conductivity, and rock specific heat remain constant. The latter two parameters do not vary significantly over the range measured in typical alluvial sediments.

Table 3. Comparison of "Current" Moisture Fluxes (in  $\text{mm yr}^{-1}$ ) for the Base Case Estimated Using a CMB Approach and the DASH Model Results\*

	CMB Liquid Flux	DASH Model Liquid Flux	DASH Model Isothermal Vapor Flux	DASH Model Thermal Vapor Flux	DASH Model Net Moisture Flux
Subroot zone (5 m depth)	-1.0	<0.001	0.007	0.009	0.016
Water table interface	-10.0	-0.044	<0.001	0.013	-0.032

\*Negative values indicate downward fluxes.

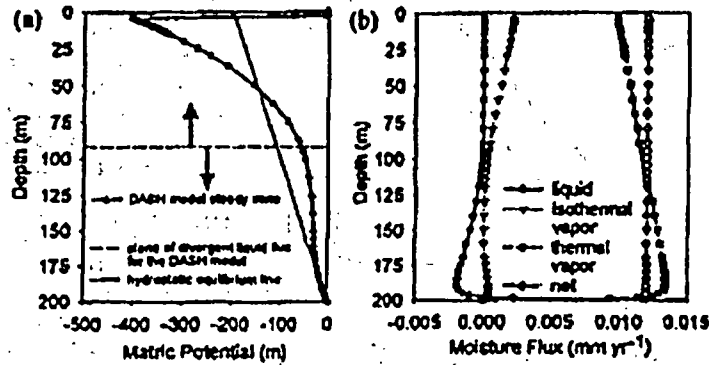


Figure 7. Comparison of steady state  $\psi$  profiles predicted by the DASH model and the linear  $\psi$  profile described by the conventional hydrostatic equilibrium model. The unit gradient model (not shown here; see example in Figure 1b) predicts a uniform  $\psi$  profiles below the root zone. (b) Steady state moisture flux profiles predicted by the DASH model. Negative values indicate downward fluxes.

[26] Simulation results in the form of steady state  $\psi$  profiles show little variation among the three soil types (Figure 10). However, the response times vary dramatically (Table 5). The simulated sand responds faster than the silt and silty clay systems for several reasons. Mainly, the higher saturated permeability of the sand, relative to the silt and silty clay, contributes to a shorter time required for the thick vadose zone to drain and equilibrate to the specified dry condition below the root zone. Simulation results generated by varying the saturated permeability over several orders of magnitude for the sand confirm the importance of liquid permeability on deep vadose zone drying response times (Table 5). The drier antecedent ( $t \leq 0$ ) moisture conditions for the sand relative to the finer-grained soil types also favors a faster response in the sand, since less moisture needs to be removed to reach the new steady state. However, this factor appears to be secondary to permeability in controlling the response time. Simulations in which we vary

the porosity from 0.2 to 0.6 (but without changing saturation or tortuosity) showed that response times decrease only slightly with decreasing porosity (Table 5). To attain a dry steady state, a soil with low porosity requires less moisture removal than does a soil with high porosity. The reduction in moisture removal overrides the decrease in vapor flux connected with the reduced gas-phase volume of the lower porosity materials.

3.3. Water Table Depth

[27] Since the water table serves as the lower boundary in the DASH model, the depth to water table strongly affects the type of moisture flux regime that develops in desert vadose zones. Figure 11 displays results from a series of DASH model simulations for water table depths ranging from 25 m to 400 m. The model-generated  $\psi$  profiles for vadose zone thicknesses of 25, 50, and 100 m show decreased curvature with increased vadose zone thickness, reflecting the decreased overall  $\psi$  gradient (Figure 11a). Vadose zones with thicknesses exceeding 100 m exhibit little sensitivity to increases in water table depth, as shown by their overlapping  $\psi$  profiles (Figure 11b), similar net upward steady state fluxes (Figure 12), and identical response times (Table 5). The steady state divergent liquid flux pattern described in section 2.6 does not develop for simulations in which the water table is >100 m deep (Figure 12). This observation is consistent with the 92-m depth of the plane of divergence for the 200-m vadose zone base case simulation. Still, vapor transport dominates the steady state moisture flux regime for water table depths exceeding 25 m. The upward vapor flux generally exceeds the upward liquid flux by at least an order of magnitude for thick (>25 m) desert

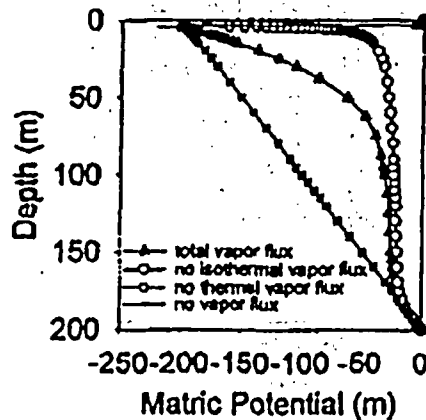


Figure 8. Comparison of steady state  $\psi$  profiles predicted when both isothermal and thermal vapor transport are included (DASH, triangles), only thermal vapor flux is included (circles), only isothermal vapor flux is included (squares), and without vapor flux (linear profile with crosses).

Table 4. Parameters Used in the Sensitivity Analysis for Three Soil Types

Soil Type	Saturated Permeability	van Genuchten Soil Parameters $\alpha, n$	Residual and Maximum Saturations
Sand	$1 \times 10^{-11} \text{ m}^2$	$4.5 \text{ m}^{-1}, 1.9$	10%, 96%
Silt	$8 \times 10^{-10} \text{ m}^2$	$1.6 \text{ m}^{-1}, 1.4$	8%, 96%
Silty clay	$7 \times 10^{-12} \text{ m}^2$	$0.5 \text{ m}^{-1}, 1.1$	16%, 96%

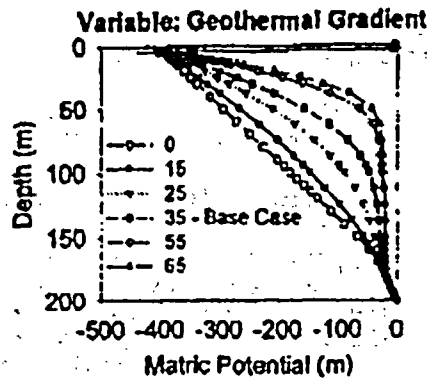


Figure 9. Steady state  $\psi$  profiles for variable geothermal gradient using the DASH model.

vadose zones. In contrast, the upward liquid flux exceeds the upward vapor flux below 10 m for the simulation in which the water table is at a depth of 25 m (Figure 12). Capillarity draws enough water upward from the water table in thinner vadose zones to significantly increase the unsaturated permeability, and consequently increase the net upward moisture flux. Model-calculated equilibrium response times reflect the influence of the water table on the flow regime for thinner vadose zones (Table 5). Response times are very short for thin vadose zones but increase rapidly with increasing thickness and reach an asymptotic value of about  $\sim 80$  kyr for vadose zones thicker than about 150 m.

#### 3.4. Fixed Subroot Zone Matric Potential

[28] Vegetation type and soil moisture availability strongly control the matric potential that fine plant roots must sustain within the root zone to survive. A series of simulations in which the fixed subroot zone  $\psi$  is varied illustrates the sensitivity of the steady state flow regime and response times to the fixed  $\psi$  value. Response times decrease with increasing (less negative) subroot zone  $\psi$  (Table 5). Although the driving force in the upper part of the profile decreases with increasing subroot zone  $\psi$  values, the steady state  $\psi$  profiles are closer to the initial  $\psi$  profile (Figure 13). Less moisture needs to be removed from the profiles maintained by less negative subroot zone  $\psi$  to attain steady state, thereby requiring less time for equilibration. However, a point is reached (at about  $-500$  m for this set of simulations) at which increasingly negative subroot zone  $\psi$  values have very little effect on the equilibrium response time (Table 5). At the dry end of the range, large changes in  $\psi$  correspond to very small differences in moisture content. Therefore the amount of moisture required for removal for equilibration to a subroot zone  $\psi$  of  $-500$  m is very close to the amount for subroot zone  $\psi < -500$  m.

#### 3.5. Enhanced Vapor Diffusion

[29] Water vapor fluxes result from spatial variations in vapor density, which is a function of both temperature and matric potential. Vapor diffusion, described by Fick's Law, becomes increasingly important to the overall transport of moisture as the porous medium dries. Laboratory

experiments conducted on unsaturated material [Philip and de Vries, 1957] and at the pore scale [Silverman, 1999] report vapor diffusion rates that exceed the rate predicted by Fick's Law. Philip and de Vries [1957] hypothesized that this vapor diffusion enhancement is primarily due to the presence of liquid islands in partially saturated porous media, where vapor is transferred essentially instantaneously from one side of the liquid island to the next. We explore the influence of enhanced vapor diffusion on response times by varying a vapor diffusion enhancement factor,  $\beta$ , from 0.5 to 10, although  $\beta > 4$  is probably unlikely under field conditions [Silverman, 1999]. Increase in  $\beta$  yield reduced response times (Table 5), emphasizing

Table 5. Summary of Equilibrium Response Times Calculated From DASH Model Sensitivity Analysis

Variable	Response Time, ky
Soil type	
Sand <sup>a</sup>	80
Silt	400
Silty clay	250
Saturated permeability $k_{sat}$ ( $m^2$ )	
$10^{-9}$	32
$10^{-10}$	59
$10^{-11}$	80
$10^{-12}$	175
$10^{-13}$	275
Porosity $\phi$ (dimensionless)	
0.2	65
0.3	72
0.4	77
0.45 <sup>b</sup>	80
0.5	82
0.6	87
Geothermal gradient $dT/dz$ ( $^{\circ}C km^{-1}$ )	
0	230
15	184
25	143
35 <sup>c</sup>	80
45	57
55	41
65	29
Water table depth $z_{wt}$ (m)	
25	0.24
50	11
100	47
150	80
200 <sup>d</sup>	80
400	80
Fixed root zone matric potential $\psi_{rs}$ (m)	
-50	31
-100	45
-200	66
-400 <sup>e</sup>	80
-600	87
-800	88
Vapor diffusion enhancement factor $\beta^f$	
0.5	122
0.75	97
1.0 <sup>g</sup>	80
2.0	55
3.0	44
4.0	37
5.0	30
10	16

<sup>a</sup> Denotes value used in base case.

<sup>b</sup> Factor relative to vapor diffusion rate described by Fick's Law; value  $> 1$  correspond to "enhanced" vapor diffusion.

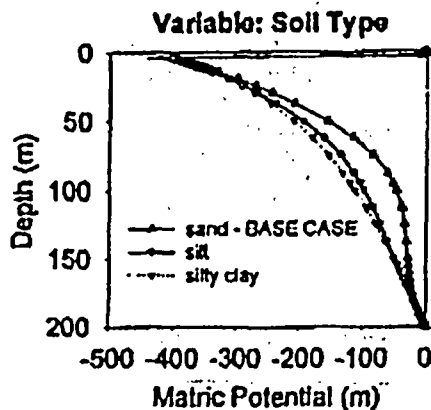


Figure 10. Steady state  $\psi$  profiles for variable soil type using the DASH model. Soil texture properties are provided in Table 3. Other base case parameters are given in Table 1.

the strong control of vapor transport on moisture redistribution in deep vadose zones undergoing drying, particularly in the later stages.

### 3.6. Summary of Sensitivity Analysis

[30] Results from the sensitivity analysis suggest that the DASH conceptual model applies to a broad range of thick, unconsolidated vadose zones under desert vegetation in interdrainage regions. Similar liquid and vapor flux patterns develop in desert vegetated vadose zones with deep water tables for a large range of variables. With the exception of relatively thin (<50 m) vadose zones, the hydraulic drying response time exceeds the timescale of major climate change. Although the hydraulic role of desert vegetation is arguably the key component in the DASH conceptual model, the sensitivity analysis results indicate that the magnitude of the subroot zone matric potential (-50 m to -800 m tested) contributes only a minor influence on the moisture flux regime and response to drying. Soil hydraulic parameters, particularly the saturated permeability, exert the strongest influence on early time drying when a large percentage of the drying is accommodated by gravity drainage. Parameters related to vapor movement, such as geothermal gradient and vapor enhancement, exert a major

control on late time drying when most of the moisture redistribution is in the vapor phase.

### 4. Transition Reversal and Response to Episodic Infiltration

[31] The sensitivity results described above demonstrate that under a range of typical conditions and soil parameters, thick alluvial desert vadose zones respond slowly to a change in surface boundary conditions representative of a transition from a mesic to an arid climate and establishment of xeric vegetation. We expect the response in the reverse direction to be considerably faster. In order to evaluate the response in desert vadose zones to a prolonged period of infiltration, we simulate several transition reversals (dry-to-wet shifts). The response to a short-lived episodic infiltration event is also addressed by simulating a dry-to-wet-to-dry sequence. Specifically, we are interested in the behavior of the pulse of infiltrating water as it propagates with depth, and the time required for  $\psi$  profiles to equilibrate to the change in the upper boundary conditions. The infiltration event simulation addresses the wetting and drying behavior in the upper vadose zone and the time required to reestablish the pre-infiltration  $\psi$  profile.

[32] The initial condition for the dry-to-wet transitions illustrated in Figures 14a and 14b consists of the dry steady state base case solution (from Figure 7). This initial condition serves to bound the high end of calculated response times. Another initial condition (not illustrated in Figure 14) we use is that established after 15 kyr of drying (see Figures 4c and 6). The boundary condition for the wetting period in the simulations consists of a specified downward liquid flux ranging from 1 to 10 mm yr<sup>-1</sup>. Table 6 records the initial and boundary condition combinations and the corresponding simulation response times. As for the previous transient simulations, we define the response time by an e-fold change in the  $\psi$  profile from initial to final states. In all dry-to-wet simulations, the system responds rapidly (Table 6) compared to the wet-to-dry transitions for the base case (80 kyr, Table 5). The shift to wetter conditions yields response times ranging from 50 yrs. for the 10 mm yr<sup>-1</sup> infiltration rate applied to the initial condition representing 15 kyrs of drying, to 375 years, for the 1 mm yr<sup>-1</sup> infiltration rate applied to the dry steady state initial condition. The  $\psi$  profiles developed after various "wetting" times suggest that even relatively short periods of infiltra-

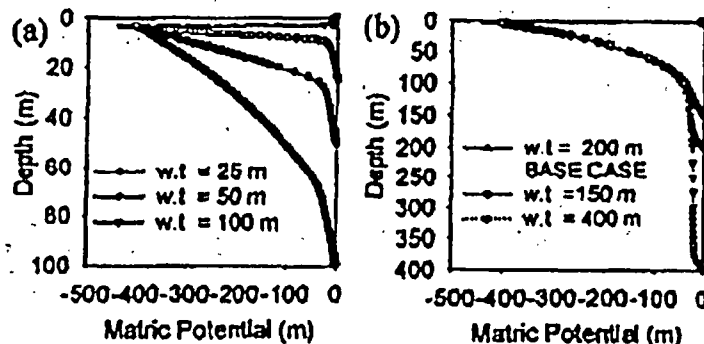


Figure 11. Steady state  $\psi$  profiles for variable water table depths of (a) 25-100 m and (b) 150-400 m.

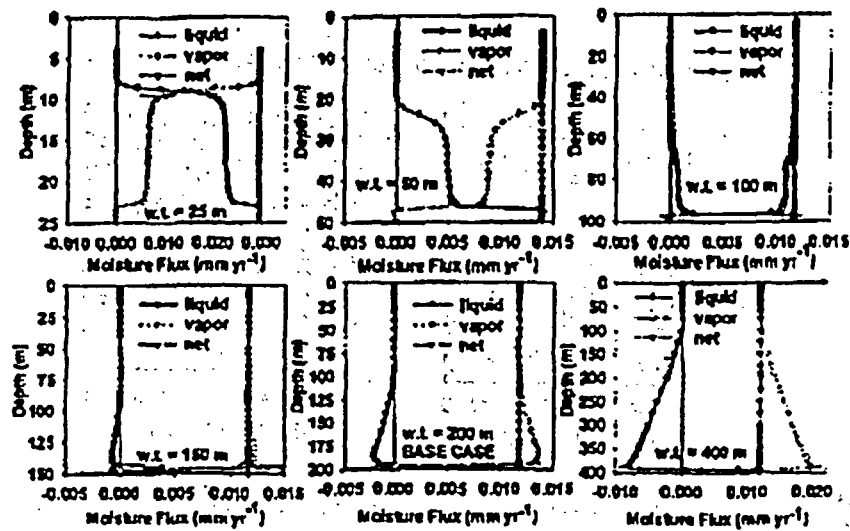


Figure 12. Steady state liquid, vapor (isothermal and thermal), and net moisture flux profiles for variable water table depths using the DASH model. Negative values indicate downward fluxes. Note the change of scale on bottom axis for the top left graph and the bottom right graph.

tion past the root zone induce a significant response in  $\psi$  profiles (Figures 14a and 14b). Infiltration could be hypothesized to result from rare, episodic, climate or weather events, but the very long timescales necessary to reestablish the highly negative  $\psi$  profiles argues against such events during the Holocene in places where these negative profiles are observed. This point is emphasized by a simulation in which water infiltrates past the root zone at rate of  $5 \text{ mm yr}^{-1}$  over a period of 10 years, using the base case parameters. The initial condition for the simulation consists of that developed after 15 kyr of drying (Figure 15a). The simulation proceeds for ten years with a constant infiltration rate of  $5 \text{ mm yr}^{-1}$  at the surface. After ten years, the wetting front has propagated to a depth of about 10 meters (Figure 15a). At this point, the dry hydraulic conditions at 4 m are resumed (fixed  $\psi = -400 \text{ m}$ ) and the profile reequilibrates (Figure 15b). Reestablishment of the preinfiltration profile requires 5000 years of persistent drying.

### 5. Implications

(1) The DASH model challenges some of the conventional conceptual models of vadose zone flow and transport as applied to arid to semiarid regions. Questioned assumptions include (1) the current flow regime in deep vadose zones can be described by a small downward advective flux (reduced-recharge model) or a hydrostatic condition (zero-recharge model) and (2) vapor fluxes are negligible compared to liquid fluxes in deep vadose zones. The DASH conceptual model proposes that the major most recent climate change at 12–15 ka had a larger impact on the vadose zone hydrology of the arid and semiarid southwestern U.S. than has previously been considered. At least in interdrainage desert-floor environments, the change to drier climate and associated shift to more xeric vegetation actually reversed moisture fluxes just below the root zone, from downward to upward. This has

major implications for contaminant migration and environmental tracer studies in arid vadose zones.

(2) Quantifying diffuse recharge by estimating liquid fluxes below the root zone and assuming that they are equivalent to groundwater recharge, i.e., fluxes across the water table interface, may not be applicable in semiarid and arid regions. The work described in this paper suggests that not only are moisture fluxes just below the root zone unequal to recharge, they may be opposing even in direction. Furthermore, downward moisture fluxes across the water table (as drainage of Pleistocene-age water) estimated using the DASH model are several orders of magnitude smaller than estimates obtained by using the CMB approach. This implies a negligible contribution to groundwater recharge through desert floors in interdrainage areas and supports the idea that, in the absence of preferential flowpaths, a thick desert vadose zone serves as an effective

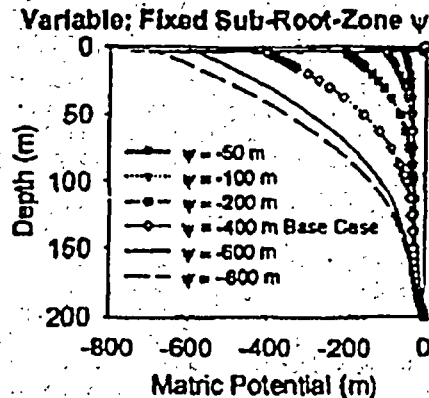


Figure 13. Steady state profiles for variable fixed subroot zone  $\psi$  values (at a depth of 4 m) using the DASH model.

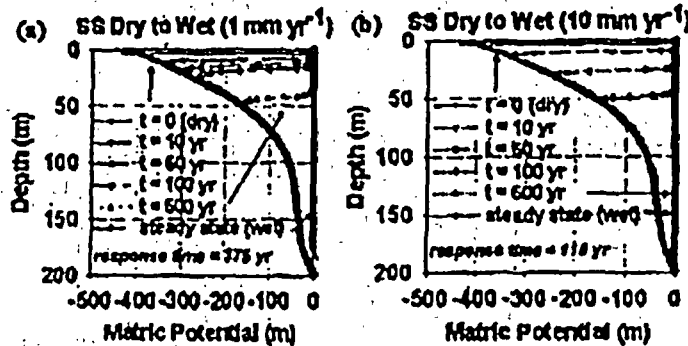


Figure 14. Transient  $\psi$  profiles using the DASH model and recording the switch from the base case dry steady state to a specified downward flux of (a)  $1 \text{ mm yr}^{-1}$  and (b)  $10 \text{ mm yr}^{-1}$ .

barrier to groundwater. However, since desert vegetation is critical in maintaining upward fluxes below the root zone, the presence or absence of native vegetation, and the ability to maintain a vegetated condition, must be considered in waste repository site assessment and emplacement procedure strategies.

## 6. Conclusions

[3] Integrating field observations with model simulations emphasizes the importance of considering both liquid and vapor flow processes when determining the magnitude and direction of moisture fluxes below the root zone. The ability to reliably make such determinations is critical to quantifying recharge beneath native desert vegetation and to assessing contaminant-transport risks. Modeled fluxes can be extremely useful in interpreting field-measured matric potential and chloride profiles that, we propose, have evolved since the Pleistocene/Holocene climate transition.

[4] The Deep Arid System Hydrodynamic (DASH) model reconciles the paradox between upward hydraulic potential gradients measured in arid and semiarid vadose zones and the downward liquid flow assumption applied when the chloride mass balance approach is used to interpret corresponding chloride profiles. The DASH model prescribes a constant low  $\psi$  just below the root zone. The presence of this persisting sink in the system, which is supported by field data, implies that desert vegetation effectively intercepts all downward infiltrating precipitation and draws much of the preexisting moisture from the upper vadose zone. With time, the upward thermal vapor flux, driven by the geothermal gradient, dominates the hydrodynamics of the deep vadose zone. The gravitationally driven return of the liquid water that results from the cooling and condensation of upward moving vapor produces the characteristic nearly uniform matric-potential profile of the deeper vadose zone. In actuality, this steady state condition may be rarely achieved in deep vadose zone regimes since response times generally exceed the typical timescale of major climate change. More likely, desert vadose zones are locked in long-term drying transients that are so gradual that they appear to be at steady state. The DASH model results suggest that current net moisture fluxes below desert root zones are generally upward, groundwater recharge is extremely small, and the net

moisture flux below the root zone is not equivalent in magnitude or direction to the flux across the water table.

## Appendix A: FEHM Model Description

[5] The models and solution algorithms for FEHM are described in detail by Tseng and Zyvoloski [2000] and Zyvoloski et al. [1997]. In this study, one dimensional columns are simulated with finite element grids of variable vertical spacing. Each system considered is modeled with a  $500 (2 \times 250)$  node, 249 rectangular element grid. Increased resolution is supplied near boundaries and coarser resolution is provided elsewhere. The boundaries on these grids are applied as follows. The pressures on bottom boundary nodes are fixed at atmospheric pressure to represent water table conditions. A constant mass flux of water at the upper boundary nodes serves as a continuous fluid source and represents either precipitation or effective precipitation, case specific. Here, effective precipitation refers to the residual soil water flux, (i.e., precipitation minus evapotranspiration). A specified solute concentration at the source node(s) (upper boundary) produces a constant solute flux. Fixed temperatures at the top and bottom boundaries establish a heat flux that is uniform through the vertical column for the examples provided in this study, since the low fluid flow rates do not significantly perturb the resulting linear temperature profile. A low matric potential is applied to the nodes 3–4 m below the surface and serves as a sink for water to represent the subroot zone hydraulic conditions. The sink nodes take up all water percolating down from the surface,

Table 6. Summary of Equilibrium Response Times Calculated From the DASH Model Transition Reversal Simulations Using the Base Case Parameters\*

Initial Condition	Upper Boundary Condition Downward Flux	Response Time, years	Shown in Figure 14
Dry steady state	$1 \text{ mm yr}^{-1}$	375	14a
Dry steady state	$5 \text{ mm yr}^{-1}$	170	
Dry steady state	$10 \text{ mm yr}^{-1}$	110	14b
15 kyr dry transient state	$1 \text{ mm yr}^{-1}$	175	
15 kyr dry transient state	$5 \text{ mm yr}^{-1}$	60	
15 kyr dry transient state	$10 \text{ mm yr}^{-1}$	50	

\*See Table 1.

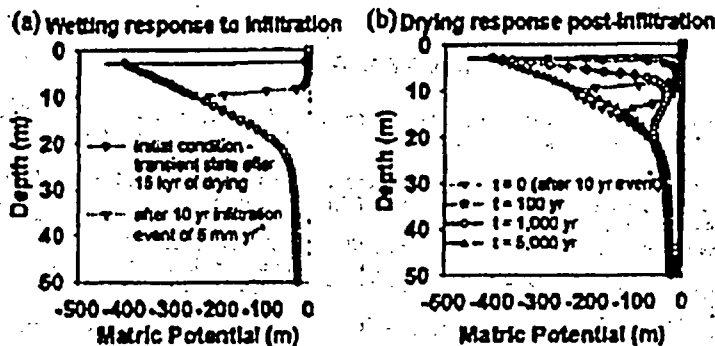


Figure 15. Transient  $\psi$  profiles using the DASH model and recording the (a) wetting response from the 15 kyr dry transient state to a 10-yr infiltration of  $5 \text{ mm yr}^{-1}$  and (b) the drying response subsequent to the infiltration event.

and draw water from below as well, but do not serve as a solute sink. The solute species is prevented from exiting the system through the subroot zone sink nodes in FEHM. This specification is critical for simulating chloride behavior.

[38] The conservation of water mass, fluid-medium energy, and noncondensable gas mass equations are solved in a quasi-coupled formulation with the solute mass transport equations. Namely, the transport equations use the flow rates and temperatures obtained in the heat- and mass transfer solution at each time step. Therefore fully coupled flow and transport (without feedback from the transport solution) is approximated by using small time steps in the simulations. Some of the unique modeling components implemented in this study include enhanced water vapor diffusion, vapor pressure lowering, and moisture-dependent solute diffusion. In FEHM, the molecular diffusivity of water vapor in air,  $D_{wv}$ , is given by:

$$D_{wv} = \tau \theta D_{wv}^0 \frac{0.101325}{P} \left[ \frac{T + 273.15}{273.15} \right]^\omega$$

where  $\tau$  is tortuosity factor,  $\theta$  is volumetric vapor content, and  $D_{wv}^0$  is the value of  $D_{wv}$  at standard conditions,  $\rho_v$  is vapor density,  $T$  is temperature, and  $P$  is pressure. The value of  $D_{wv}^0$  is set to  $2.4 \times 10^{-5} \text{ m}^2 \text{ s}^{-1}$ ,  $\omega$  is set to 2.334, and the tortuosity factor is an input parameter. Increasing the tortuosity factor above the standard value of 0.66 is used to simulate vapor diffusion enhancement as described by Phillips and DeVries [1957]. A vapor pressure lowering routine in FEHM allows for isothermal vapor transfer, i.e., vapor density dependence on pressure. The modified vapor pressure is given by:

$$P_w^*(T, P_{cap}) = P_w(T) \exp\left(-\frac{P_{cap} M_w}{\rho_w R (T + 273.15)}\right)$$

where  $P_w^*$  is the new vapor pressure of water,  $P_{cap}$  is the capillary pressure,  $M_w$  molecular mass of water,  $\rho_w$  is the density of water, and  $R$  is the gas constant. In the solute transport equations, FEHM uses a standard mathematical formulation for the solute dispersion coefficient,  $D_{11} = D_c = D_{AB} + \alpha_L v$ , where  $D_{AB}$  is molecular solute diffusion coefficient,  $\alpha_L$  is dispersivity,  $v$  is the Darcy velocity

computed from the solution of the fluid flow equation. In this study, a moisture-dependent  $D_{AB}$ , based on the function developed in Conca and Wright [1992], is employed.

[39] All simulations conducted in this study use FEHM's standard pure implicit formulation (backward-in-time Euler) for discretization of the time derivatives. Upstream weighting is used in the spatial discretization using FEHM's finite-volume formulation. Full detail on the linear equation solver (e.g., the generalized minimum residual method) is provided by Tseng and Zyvoloski [2000] and Zyvoloski et al. [1997].

[40] Acknowledgments. This research was funded by the National Science Foundation (grant EAR-9614509 (FMP) and NSF Graduate Research Fellowship (MAW)). This material is based upon work supported in part by SAHRA (Sustainability of semi-Arid Hydrology and Riparian Areas) under the STC Program of the National Science Foundation, agreement EAR-9876800. The authors wish to thank George Zyvoloski, Phillip Stauffer and Bruce Robinson from Los Alamos National Laboratory who provided invaluable assistance with FEHM modeling.

## References

- Allen, B. D., and R. Y. Anderson. Evidence from western North America for rapid shifts in climate during the Last Glacial Maximum. *Science*, 260, 1920-1923, 1993.
- Allison, G. B., A review of some of the physical, chemical, and isotopic techniques available for estimating groundwater recharge. In *Estimation of Natural Groundwater Recharge*, edited by I. Simmers, pp. 49-72. D. Reidel, Norwell, Mass., 1988.
- Allison, G. B., G. W. Gee, and S. W. Tyler. Vadose-zone techniques for estimating ground-water recharge in arid and semiarid regions. *Soil Sci. Soc. Am. J.*, 58, 6-14, 1994.
- Andraski, B. J., Soil-water movement under natural-site and waste-site conditions: A multiple-year field study in the Mojave Desert, Nevada. *Water Resour. Res.*, 33, 1901-1916, 1997.
- Bear, J., *Dynamics of Fluids in Porous Media*. Dover, Mineola, N. Y., 1972.
- Benson, L. V., D. R. Curry, R. I. Dorn, K. R. Lajoie, C. G. Oviatt, S. W. Robinson, G. I. Smith, and S. Sime. Chronology of expansion and contraction of four Great Basin lake systems during the past 35,000 years. *Paleogeogr. Paleoclimatol. Paleoecol.*, 78, 241-246, 1990.
- Blankenship, R. K., and J. E. Weir. Geohydrology of the eastern part of Pahre Mesa, Nevada Test Site, Nye County, NV. *U. S. Geol. Surv. Prof. Pap.*, 712-B, 35 pp., 1973.
- Canadell, J., R. B. Jackson, and J. R. Ehleringer. Maximum rooting depth of vegetation types at the global scale. *Oecologia*, 108, 583-593, 1996.
- Cooca, J. L., and J. Wright. Diffusion and flow in gravel, soil, and whole rock. *Appl. Hydrogeol.*, 1, 5-24, 1992.
- Cook, P. G., W. M. Edmunds, and C. B. Geyer. Estimating paleorecharge and paleoclimatic from unsaturated zone profiles. *Water Resour. Res.*, 38, 2721-2731, 1992.

- Dettinger, M. D., Reconnaissance estimates of natural recharge to desert basins in Nevada, USA, by using chloride-mass balance calculations, *J. Hydrol.*, 106, 55-67, 1989.
- Enfield, C. G., J. J. C. Hsieh, and A. W. Warrick, Evaluation of water flux above a deep water table using thermocouple psychrometers, *Soil Sci. Soc. Am. Proc.*, 37, 968-970, 1973.
- Fischer, J. M., Sediment properties and water movement through shallow unsaturated alluvium at an arid site for disposal of low-level radioactive wastes near Beatty, Nye County, Nevada, U.S. Geol. Surv., *Water Resour. Invest. Rep.*, 92-4032, 48 pp., 1992.
- Gardner, W. R., Water uptake and salt distribution patterns in saline soils, in *Isotope and Radiation Techniques in Soil Physics and Irrigation Studies. Proceedings of an International Symposium on Isotope and Radiation Techniques in Soil Physics and Irrigation Studies, Alzen-Provence, France*, pp. 335-340, Int. Atomic Energy Agency, Vienna, 1967.
- Ge, G. W., and R. R. Kirkham, Arid site water balance: Evapotranspiration modeling and measurements, *Rep. PNL-5177*, 38 pp., Pac. Northwest Lab., Richland, Wash., 1984.
- Ge, G. W., P. J. Wierenga, B. J. Andraski, M. H. Young, M. J. Fryer, and M. L. Rockhold, Variations in water balance and recharge potential at three western desert sites, *Soil Sci. Soc. Am. J.*, 58, 63-72, 1994.
- Gina, T. R., and E. M. Murphy, A transient flux model for convective infiltration: Forward and inverse solutions for chloride mass balance studies, *Water Resour. Res.*, 33, 2065-2079, 1997.
- Hillel, D., *Fundamentals of Soil Physics*, Academic, San Diego, Calif., 1980.
- Jobstson, C., Preferred water flow and localised recharge in a variable regolith, *J. Hydrol.*, 94, 129-142, 1987.
- Junga, C. E., and R. T. Werby, The concentration of chloride, sodium, potassium chloride and sulfate in rain water over the United States, *J. Meteorol.*, 15, 417-425, 1957.
- Jury, W. A., W. R. Gardner, W. H. Gardner, *Soil Physics*, John Wiley, New York, 1991.
- Koorevaar, F., G. Menclik, and D. Dirksen, *Elements of Soil Physics*, 3rd ed., Elsevier Sci., New York, 1983.
- Looney, B., and R. Falta (Eds.), *Vadose Zone Science and Technology Solutions*, vol. 1, Battelle, Columbus, Ohio, 2000a.
- Looney, B., and R. Falta (Eds.), *Vadose Zone Science and Technology Solutions*, vol. II, Battelle, Columbus, Ohio, 2000b.
- Milly, P. C., Effects of thermal vapor diffusion on seasonal dynamics of water in the unsaturated zone, *Water Resour. Res.*, 32, 509-518, 1996.
- Morrison, R. B., Quaternary stratigraphic, hydrologic, and climate history of the Great Basin, with emphasis on Lakes Lahontan, Bonneville and Tecopa, in *Quaternary Nonglacial Geology: Conterminous U.S., The Geology of North America*, vol. K-2, edited by R. B. Morrison, pp. 283-320, Geol. Soc. of Am., Boulder, Colo., 1991.
- Murphy, E. M., T. R. Gina, and J. L. Phillips, Geochemical estimates of paleorecharge in the Páscua Basin: Evaluation of the chloride mass balance technique, *Water Resour. Res.*, 32, 2853-2868, 1996.
- National Research Council, *Ward Valley: An Examination of Seven Issues in Earth Sciences and Ecology*, Natl. Acad. Press, Washington, D. C., 1995.
- Nirama, J., D. A. Stoenstrom, and K. A. Alstina, The feasibility of recharge rate determination using the steady-state centrifuge method, *Soil Sci. Am. J.*, 58, 49-56, 1994.
- Odening, W. R., B. R. Strain, and W. C. Oechel, The effect of decreasing water potential on net CO<sub>2</sub> exchange of intact desert shrubs, *Ecology*, 55, 1086-1095, 1974.
- Philip, J. R., and D. A. de Vries, Moisture movement in porous materials under temperature gradients, *Eos Trans. AGU*, 38, 222-228, 1957.
- Phillips, F. M., Environmental tracers for water movement in desert soils of the American southwest, *Soil Sci. Soc. Am. J.*, 58, 15-24, 1994.
- Phillips, F. M., A. R. Campbell, C. Kruger, P. Johnson, R. Roberts, and E. Kryes, A reconstruction of the water balance in western United States lake basins to climate change, *Rep. 269*, N. M. Water Resour. Res. Inst., Las Cruces, 1992.
- Priehman, W. T., J. S. Sperry, and J. W. O'Leary, Sustained and significant water pressure in xylem, *Nature*, 378, 715-716, 1995.
- Prudic, D. E., Estimates of percolation rates and ages of water in unsaturated sediments at two Mojave Desert sites, California-Nevada, U.S. Geol. Surv. *Water Res. Invest. Rep.*, 94-1160, 19 pp., 1994.
- Pyth, E. A., Using chloride and chlorine-36 as soil-water tracers to estimate deep percolation at selected locations on U.S. Department of Energy Hanford site, Washington, U.S. Geol. Surv. *Water Supply Paper*, 2481, 67 pp., 1998.
- Reid, C. C., and B. M. Thompson (Eds.), *Deserts as Dumps? The Disposal of Hazardous Materials in Arid Ecosystems*, Univ. of N. M. Press, Albuquerque, 1992.
- Reid, B., A conceptual model of deep unsaturated zone with negligible recharge, *Water Resour. Res.*, 20, 1627-1629, 1984.
- Scanlon, B., Evaluation of moisture flux from chloride data in desert soils, *J. Hydrol.*, 128, 137-156, 1991.
- Scanlon, B. R., Uncertainties in estimating water fluxes and residence times using environmental tracers in an arid unsaturated zone, *Water Resour. Res.*, 36, 395-409, 2000.
- Scanlon, B. R., and R. S. Goldsmith, Field study of spatial variability in unsaturated flow beneath and adjacent to playas, *Water Resour. Res.*, 33, 2239-2252, 1997.
- Scanlon, B. R., S. W. Tyler, and P. J. Wierenga, Hydrologic issues in semi-arid, unsaturated systems and implications for contaminant transport, *Rev. Geophys.*, 33, 461-490, 1997.
- Scanlon, B. R., R. P. Langford, and R. S. Goldsmith, Relationship between geomorphic settings and unsaturated flow in an arid setting, *Water Resour. Res.*, 35, 983-999, 1999.
- Schaefer, C. E., R. R. Aranda, H. A. van der Sloot, and D. S. Korson, Prediction and experimental validation of liquid-phase diffusion resistance in unsaturated soils, *J. Contam. Hydrol.*, 20, 145-166, 1995.
- Silverman, T., A pore-scale experiment to evaluate enhanced vapor diffusion in porous media, M.S. thesis, N. M. Inst. of Mining and Technol., Socorro, 1999.
- Stephens, D. B., A perspective on diffuse natural recharge mechanisms in areas of low precipitation, *Soil Sci. Soc. Am. J.*, 58, 40-48, 1994.
- Stephens, D. B., *Vadose Zone Hydrology*, A. F. Lewis, Boca Raton, Fla., 1996.
- Stephens, D. B., and R. K. Knowlton Jr., Soil water movement and recharge through sand at a semiarid site in New Mexico, *Water Resour. Res.*, 22, 881-889, 1986.
- Stone, W. J., Recharge in the Salt Lake Coal Field based on chloride in the unsaturated zone, *N. M. Bur. Mines Geol. Res. Open File Rep.*, 217, 64 pp., 1974.
- Stone, W. J., and B. E. McGurt, Ground-water recharge on the southern high plains, east-central New Mexico, in *New Mexico Geological Society Guidebook, 36th Field Conference*, pp. 331-335, N. M. Geol. Soc., Santa Rosa, 1985.
- Tseng, P. H., and G. A. Zyvoloski, A reduced degree of freedom method for simulating non-isothermal multi-phase flow in a porous medium, *Adv. Water Resour.*, 23, 731-745, 2000.
- Tyler, S. W., J. B. Chapman, S. H. Conrad, D. P. Hammermeister, D. O. Blout, J. J. Miller, M. J. Sully, and I. M. Ginnani, Soil-water flux in the southern Great Basin, United States: Temporal and spatial variations over the last 120,000 years, *Water Resour. Res.*, 32, 1481-1499, 1996.
- van Genuchten, M. T., A closed-form equation for predicting the hydraulic conductivity of unsaturated soils, *Soil Sci. Soc. Am. J.*, 44, 892-898, 1980.
- Walvoord, M. A., A unifying conceptual model of water, vapor and solute transport in deep arid vadose zones, Ph.D. thesis, N. M. Inst. of Mining and Technol., Socorro, 2002.
- Walvoord, M. A., F. M. Phillips, S. W. Tyler, and P. C. Hartstough, Deep arid system hydrodynamics. 2. Application to paleohydrologic reconstruction using vadose-zone profiles from the Northern Mojave Desert, *Water Resour. Res.*, 38, doi:10.1029/2001WR000825, in press, 2002.
- Wongprad, L. J., Radioactive waste storage in thick unsaturated zone, *Science*, 212, 1457-1464, 1981.
- Wood, W. W., Use and misuse of the chloride-mass balance method in estimating ground water recharge, *Ground Water*, 37, 2-3, 1999.
- Zyvoloski, G. A., B. A. Robinson, Z. V. Dash, and L. L. Trease, Summary of the models and methods for the FEHM application—A finite-element heat-and-mass-transfer code, *Rep. LA-13307-ACS*, Los Alamos Natl. Lab., Los Alamos, N. M., 1997.

F. M. Phillips, Earth and Environmental Science Department, New Mexico Institute of Mining and Technology, Socorro, NM 87801, USA.

M. A. Plummer, Idaho National Engineering and Environmental Laboratory, Idaho Falls, ID 83415, USA.

M. A. Walvoord, U.S. Geological Survey, Denver Federal Center, Box 25046, MS 412, Lakewood, CO 80223-0046, USA. (walvoord@usgs.gov)

A. V. Wolfberg, Earth and Environmental Sciences Division, Los Alamos National Laboratory, Los Alamos, NM 87545, USA.